An Analysis of Minimally Perturbing Temperature Probe and Thermographic Measurements in Microwave Diathermy

CHRISTIAN U. HOCHULI AND GIDEON KANTOR, SENIOR MEMBER, IEEE

Abstract—**Temperature measurements in fat–muscle phantoms using thermography and a minimally perturbing temperature probe were investigated. Two microwave applicators (915- and 2450-MHz) were used to induce the heating in the phantom. Discrepancies between data taken with the thermographic camera versus the probe were measured. These discrepancies were shown to be primarily caused by a 40-s time delay in performing temperature measurements with the thermographic camera, which resulted in additional thermal diffusion in the phantom.**

I. Introduction

THE PURPOSE of this paper is to describe the techniques for measuring temperature in these planar, simulated, fat–muscle phantoms with a minimally perturbing temperature probe, and to compare these results against measurements made with a thermographic camera. Specifically, we were interested in the differences between the data for the measured heating depth and net power delivered to the applicator (antenna) for a given absorbed power per unit weight in simulated, human muscle tissue.

II. Theory

Once the microwave-induced temperature rise had been measured, we were able to approximately calculate the absorbed power per unit weight deposited in the phantom tissues. There is no blood flow or metabolic heating present in the synthetic human tissues, since only the electrical properties are simulated for a specific frequency and temperature range. Thus we can write down the heat transport equation

$$K\nabla^2 T-\rho C\frac{\partial T}{\partial t}=-\frac{\sigma|E|^2}{2}+P_C \qquad (1)$$

where K is the thermal conductivity of tissue (W/m·°C), T is temperature (°C), ρ is mass density of tissue (kg/m^3), C is the specific heat of tissue (W·s/kg·°C), t is time (s), σ is the electrical conductivity of tissue (℧/m), E is the rms electrical field vector (V/m), and P_C is the heat dissipated by convection (W/m^3). In our analysis we neglected the first term (thermal conduction) on the left-hand side of (1), and also the thermal convection term on the right-hand side. Rewriting (1), we can define the specific absorption rate (SAR) to be

$$\mathrm{SAR}=C\frac{\Delta T}{\Delta t} \qquad (2)$$

where ΔT is the microwave-induced temperature rise (°C), Δt is time of microwave exposure (s), and the SAR is in units of watts per kilogram [1]. By dividing the SAR by its peak value in the tissue one can obtain the normalized SAR (unitless).

III. Experimental Setup

A. Thermography

Fig. 1 shows the 915- and 2450-MHz Bureau of Radiological Health (BRH) prototype applicators used in this paper [2], [3]. These applicators were used to induce heating in a planar fat–muscle phantom with a 2-cm fat layer. The experimental setup for measuring heating patterns was described in detail in previously published papers and is shown in Fig. 2 [4], [5]. Briefly, for internal heating, the applicator is placed symmetrically on top of the planar phantom. After the phantom has been heated by either of two applicators for 10 s, one half-section of the phantom is quickly removed (to minimize thermal diffusion) so that a thermographic camera can view the internal cross-sectional heating pattern. Photographs of this heating pattern can only be consistently made 40 s after the microwave power has been shut off, because of the time necessary to open and photograph one half-section of the phantom.

B. Minimally Perturbing Temperature Probe

The same experimental setup was used, except that the planar, fat–muscle phantom did not have to be separated to obtain real-time temperature measurements both during and after microwave exposure. To accommodate a commercially available 1-mm-diameter temperature probe, a small hole was bored out of the Plexiglas side of the phantom (Fig. 3). The probe uses high-resistance leads (Fig. 4), and its sensor is a small bead thermistor [6], [7]. Table I gives additional specifications of this thermometer [6], [7]. The thermistor bead was placed at discrete points along the z-axis and the leads lay in the vertical (y–z) midplane in one half-section of the phantom (Fig. 3). The

Manuscript received April 13, 1981; revised August 7, 1981. The mention of commercial products, their sources, or their use in connection with material reported herein is not to be construed as either an actual or implied endorsement of such products by the Bureau of Radiological Health (BRH).

The authors are with the Division of Electronic Products, Bureau of Radiological Health, FDA, Rockville, MD 20857.

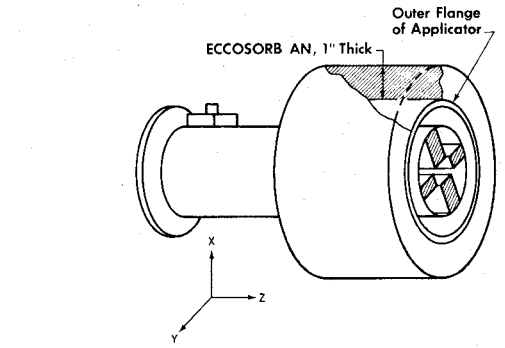

(a)

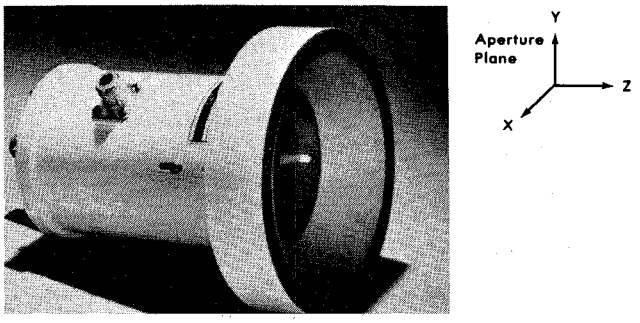

(b)

Fig. 1. (a) BRH 915-MHz circularly polarized applicator. (b) BRH 2450-MHz circularly polarized applicator.

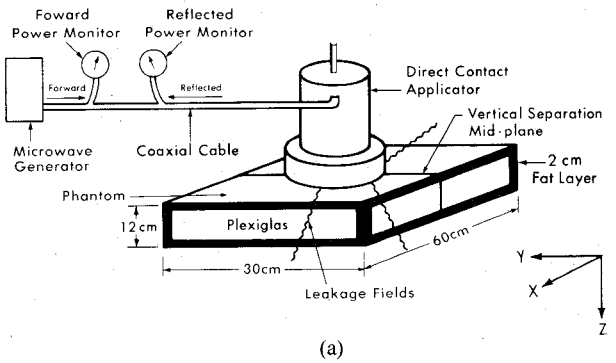

(a)

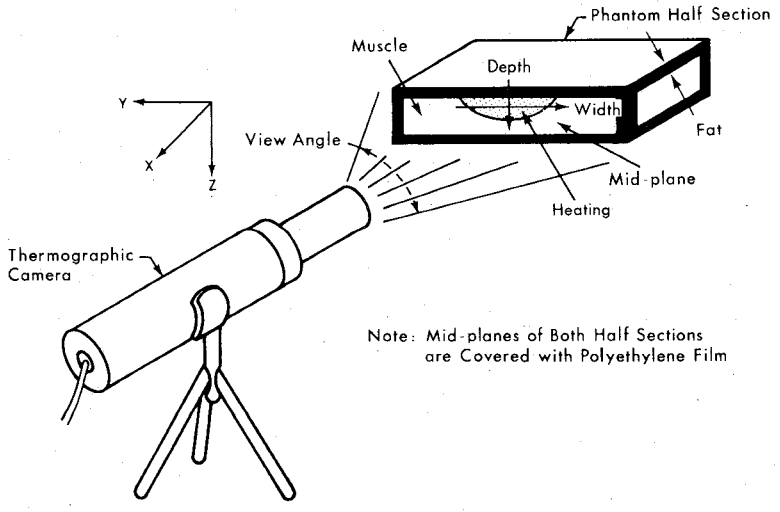

(b)

Fig. 2. Thermographic experimental setup. (a) Microwave heating. (b) Heating pattern measurement.

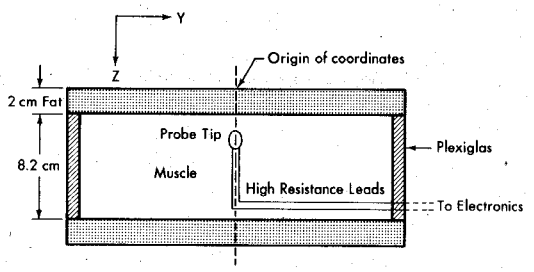

Fig. 3. Half-section of phantom with temperature probe inserted.

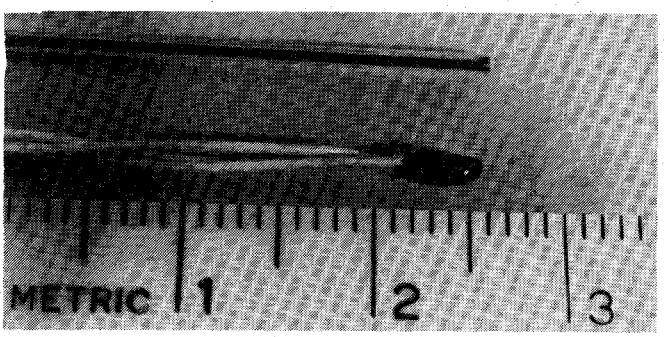

Fig. 4. From top to bottom: 1) VITEK minimally perturbing probe with high-resistance leads and thermistor sensor, 1-mm diameter; and 2) YELLOW SPRINGS INSTR. conventional temperature probe with three wire metallic leads and thermistor sensor.

TABLE I
VITEK MD. 101 ELECTROTHERMIA MONITOR SPECIFICATIONS

A.	Probe tip diameter: 1 mm
B.	Probe exponential response time, τ, including electronics: 0.74 ± 0.1 secs*.
C.	Measured thermal lag in muscle tissue when heated at 1 °C/min: approximately -0.01 °C**.
D.	Noise on output signal: less than 0.01 °C.
E.	Probe calibration at T = 25 °C, 35 °C and 45 °C: calibration uncertainty in temperature (ΔT) = ±0.01 °C**.
F.	Nonlinearity: +0.012 °C per °C from 25 °C down to 22 °C and -0.012 °C per °C from 25 °C up to 26 °C.
G.	For probe and leads aligned with the electric field vector in free space, the "near field" microwave heating of the high-resistance leads showed +0.12 °C heating for a 1 °C/min heating rise in water at 2.0 GHz**; while for a 1 °C/min heating rise with the probe in simulated muscle tissue at 2.0 GHZ, it was 0.01 °C***.

*Measured at the Bureau of Radiological Health.

**Measured by the manufacturer.

***Telephone conversation with the manufacturer.

surface of the half-section was then covered with a 0.05-mm polyethylene film. The real-time temperature response of the probe to microwave heating was plotted on a chart recorder; from this plot, the temperature rise versus heating time was determined for a constantly applied microwave power level.

IV. MEASUREMENTS

A. Thermographic Data

Figs. 5 and 7 show midplane heating patterns (whitest areas are the hottest), the upper thermogram under ambient conditions, and the lower thermogram after microwave heating. The selected temperature profiles corresponding to the white scan lines of Figs. 5 and 7 are shown in Figs. 6 and 8, respectively. Analysis of the thermographic data gives a depth of penetration "d" of 1.6 cm and 1.0 cm for the 915- and 2450-MHz applicators, respectively. The depth of penetration is defined as the distance between the fat–muscle interface and the depth at which there is a 50-percent fall off from the maximum temperature rise in the simulated muscle [5]. From SAR calculations of these data and assuming we have linearity with power, it follows that net powers of 61 and 34 W are needed (915- and

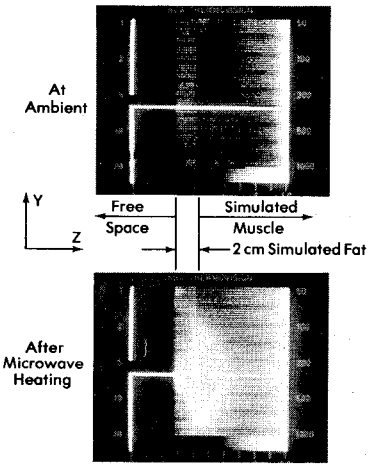

Fig. 5. Thermographic surface temperature profiles for half-section of phantom heated by BRH 915-MHz circularly polarized applicator. The top figure is the ambient profile before microwave heating and the bottom figure is after microwave heating. The horizontal white line on the top figure is the selected scan line for the profile shown in Fig. 6. The degree of heating on the bottom figure is shown by the degree of whiteness.

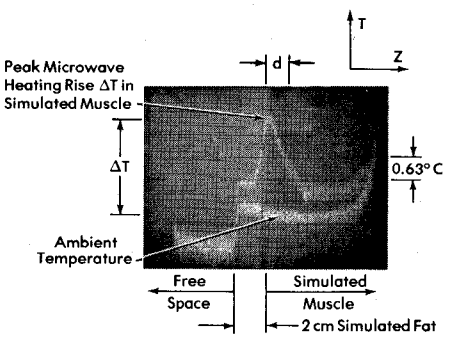

Fig. 6. Thermographic temperature depth profile for microwave-induced heating from BRH 915-MHz circularly polarized applicator. The depth profile was taken along the selected scan line shown in Fig. 5 and is actually along the z-axis of our coordinate system.

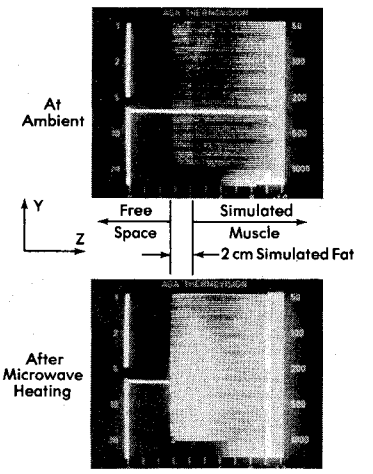

Fig. 7. Thermographic surface temperature profiles for half-section of phantom heated by BRH 2450-MHz circularly polarized applicator. The top figure is the ambient profile before microwave heating and the bottom figure is after microwave heating. Again the horizontal white line is as in Fig. 5 and the degree of heating is shown by the degree of whiteness.

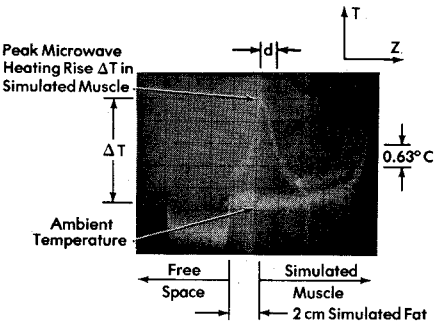

Fig. 8. Thermographic temperature depth profile for microwave-induced heating from BRH 2450-MHz circularly polarized applicator. Again the depth profile was taken along the selected scan line shown in Fig. 7 and is actually along the z-axis of our coordinate system.

2450-MHz applicators, respectively) to deliver an adequate clinical SAR of 150 W/kg to the simulated muscle tissue of the phantom [8].

B. Thermometer Probe Data

The temperature rise "T" versus time "t" was measured in the phantom, with both halves together, at a discrete set of points along the z-axis (Fig. 3). These temperature measurements were real-time and were performed during and after microwave exposure. The temperature rise, measured at the time (10 s) the microwave field was turned off, was used to calculate the normalized SAR [1], [5]. This thermometer probe has been shown to have a small amount (see Table I) of radio frequency (RF) resistance-line heating, a finite probe response time, and a small nonlinearity in the temperature response (these small errors were not included in the analysis) [6], [7]. Normalized SAR's along the z-axis (see Fig. 3) are plotted in Figs. 9 and 10 for the 915- and 2450-MHz applicators. An analysis of these curves gives depths of penetration "d" of 0.9 and 0.8 cm for the 915- and 2450-MHz applicators, respectively. From SAR calculations, it was determined that net powers of 24 and 19 W are needed (915 and 2450 MHz, respectively) to deliver an adequate clinical SAR of 150 W/kg to the simulated muscle tissue of the planar phantom.

V. Analysis

A. Depth of Penetration

From the measurement, Section IV, one can see that there are apparent discrepancies, between the data taken with the thermographic camera and the temperature probe, for the depth of penetration "d" and the net power of the applicators needed to deliver an SAR of 150 W/kg. The thermographic data show the depths of penetration to be about 78 and 25 percent larger (915 versus 2450 MHz, respectively) than that measured with the temperature probe.

These discrepancies are clearly shown in Figs. 9 and 10 where we have also plotted the thermographic data of Figs. 6 and 8. The data in the fat layer may not be reliable because of inadequate thermal and electrical contact between the two half-sections of the phantom. One source of

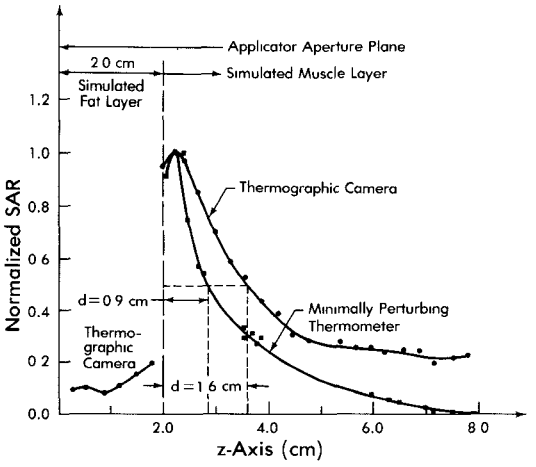

Fig. 9. Depth heating as measured by minimally perturbing temperature probe versus thermographic camera for BRH 915-MHz circularly polarized applicator.

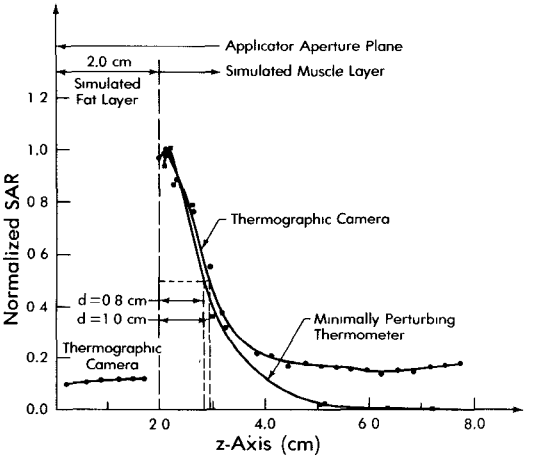

Fig. 10. Depth heating as measured by minimally perturbing temperature probe versus thermographic camera for BRH 2450-MHz circularly polarized applicator.

these discrepancies is the thermographic lens aberrations which cause large differences between the thermographic curves and the temperature probe curves (Figs. 9 and 10) for distances of z larger than about 5 cm [10]. In our case, the origin of the coordinates of the phantom are located at the center of the thermographic image. However, the discrepancies in the measured values of "d" at 915 and 2450 MHz result from the time delay of at least 40 s in opening the phantom for thermographic measurements.

During the time delay, the microwave-induced heating peak decayed through the heat transport phenomena of heat radiation and convection after opening the phantom, as well as thermal diffusion both during and after microwave heating [6], [9], [10]. To evaluate this decay, real-time probe measurements of the temperature along the z-axis were made during and after microwave heating. The normalized SAR was then calculated along the z-axis from the temperatures measured at two discrete times: immediately after 10 s of microwave heating and 40 s after the microwave power had been turned off. In both cases, the time of exposure used in the calculations was 10 s but the tempera-

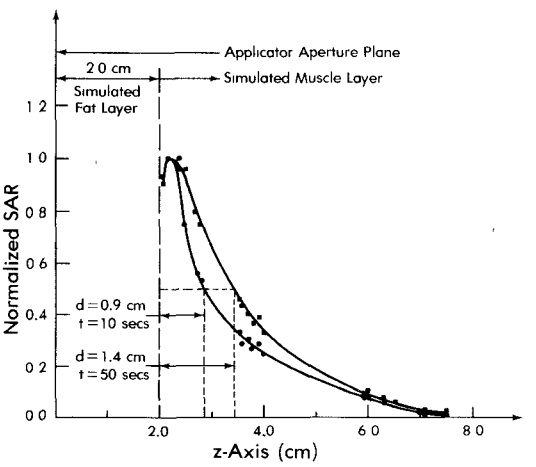

Fig. 11. Variation of the depth heating with time for the BRH 915-MHz circularly polarized applicator. Both curves were calculated from temperature measurements made at discrete points along the z-axis by a minimally perturbing temperature probe at two times: immediately after microwave heating ceased ($t=10$ s) and 40 s after microwave heating had ceased. Notice the variation in the depth of penetration "d" for the time-delayed normalized SAR curve.

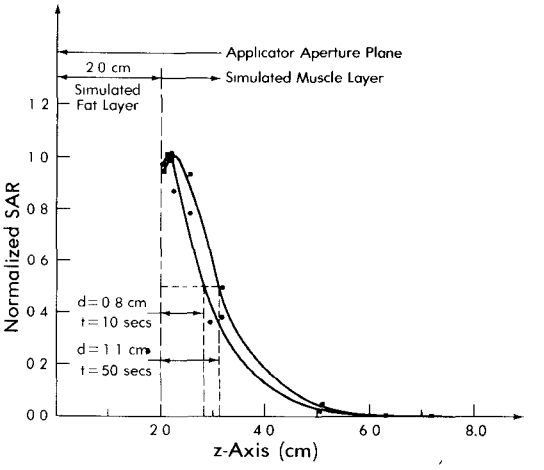

Fig. 12. Variation of the depth heating with time for the BRH 2450-MHz circularly polarized applicator. Both curves were calculated from temperature measurements made at discrete points along the z-axis by a minimally perturbing temperature probe at two times: immediately after microwave heating ceased ($t=10$ s) and 40 s after microwave heating had ceased. Again, notice the variation in the depth of penetration "d" for the time-delayed normalized SAR curve.

tures measured at the two times varied. These normalized SAR curves are drawn in Figs. 11 and 12. From these two figures, it can be seen that the delayed time curves have shifted to the right, relative to the fat–muscle interface. This shift results in a larger depth of penetration.

In fact, the time-delayed temperature probe data show almost the same depth of penetration "d" as the thermographic data. One would expect a slightly smaller value for "d" as determined by the minimally perturbing temperature probe, because there is less convective and radiative cooling when the phantom is not opened.

Also note that the calculated depth of penetration "d" for both the 915- and 2450-MHz applicators are almost the same for the temperature probe measurements taken at $t=10$ s. It has been shown theoretically and experimentally

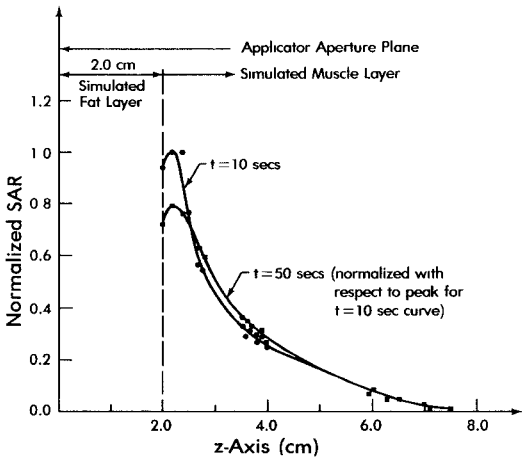

Fig. 13. Variation of the normalized SAR with time for the BRH 915-MHz circularly polarized applicator. Both curves were calculated from temperature obtained using a minimally perturbing temperature probe at the two times shown. In this case, the time-delayed curve of the normalized SAR had its peak SAR normalized relative to the peak SAR of the curve measured at time of 10 s.

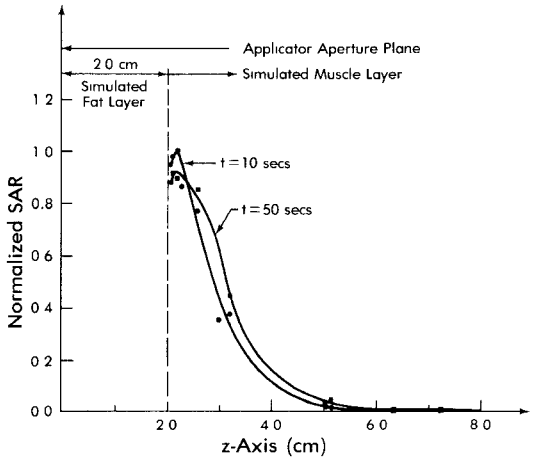

Fig. 14. Variation of the normalized SAR with time for the BRH 2450-MHz circularly polarized applicator. Again, both curves were calculated from temperatures obtained using a minimally perturbing temperature probe at the two times shown. Normalizations same as for Fig. 13.

that the calculated depth of penetration "d" increases with decreasing frequencies for plane wave sources with electrically "large" apertures from 400 to 2450 MHz [4], [12]. Physically, the measured aperture diameter of the 915-MHz applicator is almost the same as for the 2450-MHz applicator. The effective aperture diameter might really be one half of the 2450-MHz applicator aperture diameter because of ridge construction. Thus a possible reason for the low calculated depth of penetration "d" of our 915-MHz applicator compared to our 2450-MHz applicator might be the electrically "small" aperture.

B. The Net Power

For the thermographic measurements, the calculated net powers need to deliver a peak value of 150 W/kg to the muscle material are 2.5 times larger at 915 MHz and 1.8 times larger at 2450 MHz than those measured with the temperature probe. In order to explain this discrepancy we

TABLE II
SUMMARY OF DATA

Type of Applicator	915-MHz BRH circularly polarized	2450-MHz BRH circularly polarized	915-MHz Air-cooled with Ra-dome (12)
Thermographic Data*			
Depth of Penetration(cm)	1.6	1.0	1.2
Net Power** (W)	61.0	34.0	50.0
Thermometer***			
Depth of Penetration(cm)	0.9	0.8	-
Net Power** (W)	24.0	19.0	-
Theoretical			
Depth of Penetration(cm)	-	-	1.0

*Thermographic camera:
a) Spatial resolution $\geq$ 3.22 mm (10).
b) Absolute temperature uncertainty = ±0.3°C (10).

**Net power to the applicator required to deliver an adequate clinical SAR of 150 W/kg to the simulated muscle tissue of the phantom (8)

***VITEK Thermometer (See Table I):
a) Probe sensor placement ± 1 mm.
b) Absolute temperature uncertainty $\geq$ 0.03°C.

have replotted the data from Section V-A (Figs. 11 and 12) in Figs. 13 and 14. All the data for each applicator were normalized to the peak heating of the curve measured immediately after microwave power was turned off ($t = 10$ s). The curves of Figs. 13 and 14 obtained from temperature probe measurements show that the calculated net powers needed to deliver a peak value of 150 W/kg to the muscle material were 1.3 times larger at 915 MHz and 1.1 times larger at 2450 MHz when the 40-s time-delayed data were used rather than the data taken immediately. These discrepancies in the net powers were less than those noted above between the undelayed thermometer data and the 40-s time-delayed thermographic camera data. One possible reason for this is that the thermographic camera measurements were made on an opened phantom, allowing convective and radiative losses, while the temperature probe measurements were not. Table II summarizes the data, including both experimental and theoretical data on another 13-cm by 13-cm rectangular, 915-MHz contact applicator for comparison [12].

VI. Conclusion

We have shown that there can be large discrepancies in the thermographic measurements compared to minimally perturbing temperature probe measurements if a 40-s time delay exists between cessation of microwave power and the taking of the data. These discrepancies were primarily caused by the time delay in photographing the depth profile, which allows thermal diffusion to reduce the peak heating regions. However, the discrepancies in the depth of penetration "d" result mainly from the profile's definition, since the shape of the heating curve along the z-axis

changes very little with time except at the location of peak heating values. By using this knowledge, one could possibly find a better equation to calculate the depth of penetration, i.e., by neglecting the peak temperature (heating) in the analysis. Theoretically, calculated values of "d" for numerous other applicators gave excellent agreement with temperature probe values obtained immediately after microwave heating ceased, although the designs of the other applicators were different [8], [11], [12].

The net power values required to induce a given spatial SAR maximum as calculated from measurements made by the thermographic camera also differ considerably from the temperature probe values. Again, this was due to the rapid decline in the peak heating value with time. As a result, the net power equation is more critically dependent on the peak heating than the depth of penetration. This discrepancy is further increased by convective and radiative cooling due to the opening of the phantom during the thermographic measurements. A possible method of removing this discrepancy would be to use a mean value of the curve in a new equation, although some information would still be lost. The shape of the curve at the peak heating varies considerably among different applicators, object geometries, etc.

The easiest solution to these problems is to find a method for obtaining thermographic images in less than about 10 s after microwave heating has ceased, thus preventing unwanted thermal diffusion. Work is presently underway to interface the thermographic camera output to our computer, which should help remedy the problems previously discussed.

References

[1] A. W. Guy, "Physical aspects of the electromagnetic heating of tissue volume," in *Proc. Int. Symp. on Cancer Therapy by Hyperthermia and Radiation* (Washington, DC, Apr. 28–30, 1975), pp. 179–192.

[2] G. Kantor, D. M. Witters, and T. W. Greiser, "The performance of a new direct contact applicator for microwave diathermy," *IEEE Trans. Microwave Theory Tech.*, vol. MTT-26, no. 8, pp. 563–568, Aug. 1978.

[3] G. Kantor and D. M. Witters, "Comparative study of microwave diathermy at 434 MHz, 915 MHz, and 2450 MHz," to be published.

[4] A. W. Guy, J. F. Lehmann, J. A. McDougall, and C. C. Sorenson, "Studies on therapeutic heating by electromagnetic energy," in *Thermal Problems in Biotechnology*. New York: ASME 1968, pp. 26–45.

[5] G. Kantor and T. C. Cetas, "A comparative heating pattern study of direct contact applicators in microwave diathermy," *Radio Sci.*, vol. 12, no. 6S, pp. 111–120, Nov.–Dec. 1977.

[6] C. U. Hochuli, "Procedures for evaluating nonperturbing temperature probes in microwave fields," HHS Publ. FDA 81-8143, May 1981.

[7] R. R. Bowman, "A probe for measuring temperature in radio-frequency-heated material," *IEEE Trans. Microwave Theory Tech.* (Short Papers), vol. MTT-24, pp. 43–45, Jan. 1976.

[8] J. F. Lehmann, A. W. Guy, J. B. Stonebridge, and B. J. deLateur, "Evaluation of a therapeutic applicator for effective deep-tissue heating in humans," *IEEE Trans. Microwave Theory Tech.*, vol. MTT-26, no. 8, pp. 556–563, Aug. 1978.

[9] T. C. Cetas, "Temperature measurement in microwave diathermy fields: Principles and probes," in *Proc. Int. Symp. on Cancer Therapy by Hyperthermia and Radiation* (Washington, D.C., Apr. 28–30, 1975), pp. 193–203.

[10] T. C. Cetas, "Practical thermometry with a thermographic camera-calibration, transmittance, and emittance measurements," *Rev. Sci. Instr.*, vol. 49, no. 2, pp. 245–254, Feb. 1978.

[11] A. W. Guy, "Electromagnetic fields and relative heating patterns due to a rectangular aperture source in direct contact with bilayered biological tissue," *IEEE Trans. Microwave Theory Tech.*, vol. MTT-19, no. 2, pp. 214–223, Feb. 1971.

[12] A. W. Guy, J. F. Lehmann, J. B. Stonebridge, and C. C. Sorenson, "Development of a 915-MHz direct-contact applicator for therapeutic heating of tissues," *IEEE Trans. Microwave Theory Tech.*, vol. MTT-26, no. 8, pp. 550–556, Aug. 1978.

Christian U. Hochuli received the B.S. and M.S. degrees in electrical engineering from the University of Maryland College Park, in 1978 and 1980, respectively.

He is an electronics engineer at the Bureau of Radiological Health, Food and Drug Administration. His primary responsibility is to evaluate the safety and effectiveness of electronic products.Presently, he is providing technical support for evaluating short-wave and microwave diathermy antenna heating patterns in simulated human tissues. He is also the main project engineer for the Bureau's temperature calibration facility as well as evaluating procedures and performing tests on newly available minimally perturbing radio-frequency thermometers. The areas of interest include doing research into measurement of the absorbed power deposited and the radio-frequency propagation into lossy dielectrics as well as the induced heating and the heat transport mechanisms.

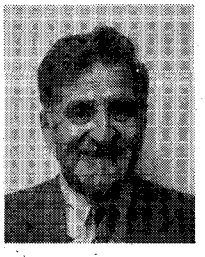

Gideon Kantor (S'46–M'50–SM'69) received the B.E.E. degree from New York University, New York, in 1948, the M.E.E. degree from the Polytechnic Institute of Brooklyn, Brooklyn, NY, in 1950, and the Ph.D. degree in electrical engineering from Cornell University, Ithaca, NY, in 1963.

He is a Physicist at the Bureau of Radiological Health, Food and Drug Administration, Bethesda, MD. His primary responsibility is to evaluate the safety and effectiveness of electronic products. Presently, he is providing technical support to the proposed microwave diathermy standard by studying the thermographic heating patterns and the associated leakage induced by direct contact applicators in simulated tissue. He is also involved in the evaluation of equipment used for microwave-induced hyperthermia treatments of cancer. His previous experience includes being a Member of Technical Staff at the MITRE Corporation, Senior Staff Scientist at the AVCO Corporation, Physicist at the Air Force Cambridge Laboratories, and Research Associate at the Microwave Research Institute, Polytechnic Institute of Brooklyn. The areas of interest were radar system studies and research in radiowave propagation as well as microwave components.

Dr. Kantor was Chairman of the Washington MTT-S Chapter during 1977-1978 and Member of the Steering and Technical Program Committees of the 1980 International Microwave Symposium. He is presently Vice-Chairman of the IEEE Washington Section and Division IV PAC Coordinator. He is a Member of the FDA Sigma Xi Club.